Accepted Manuscript

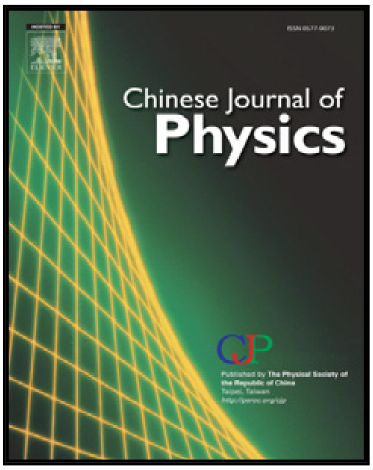

Passive control of nanoparticle due to convective heat transfer of Prandtl fluid model at the stretching surface

Feroz Ahmed Soomro , Rizwan-ul Haq , Zafar Hayat Khan , Qiang Zhang

PII: S0577-9073(17)30192-2
DOI: 10.1016/j.cjph.2017.05.007
Reference: CJPH 238

To appear in: *Chinese Journal of Physics*

Received date: 27 February 2017
Revised date: 10 May 2017
Accepted date: 10 May 2017

Please cite this article as: Feroz Ahmed Soomro , Rizwan-ul Haq , Zafar Hayat Khan , Qiang Zhang , Passive control of nanoparticle due to convective heat transfer of Prandtl fluid model at the stretching surface, *Chinese Journal of Physics* (2017), doi: 10.1016/j.cjph.2017.05.007

Highlights

- Analysis is performed for Prandtl fluid model.
- Results are analyzed for zero flux of nanoparticles at the surface.
- Convective and stagnation point effects are also incorporated within the nanofluid.
- Stream lines behavior is also described for radiation parameter.

Passive control of nanoparticle due to convective heat transfer of Prandtl fluid model at the stretching surface

Feroz Ahmed Soomro[1], *Rizwan-ul-Haq*[2,*], *Zafar Hayat Khan*[3], *Qiang Zhang* [1]

[1]*Department of Mathematics, Nanjing University, Nanjing 210093, China*

[2]*Department of Electrical Engineering, Bahria University Islamabad Campus, Islamabad, Pakistan*

[3]*Department of Mathematics, University of Malakand, Dir (Lower), Khyber Pakhtunkhwa, Pakistan*

[*]*Corresponding author: E-mail: ideal_riz@hotmail.com*

Abstract

The objective of present research work is to establish the non-Newtonian nanofluid flow and heat transfer along a stretching surface. Stagnation point flow of Prandtl nanofluid is purposed over a convective surface where zero normal flux of nanoparticles is considered to disperse the particle away from the surface. Physical problem is governed by mathematical model which consists of continuity, momentum, energy and concentration equations which are adapt to non-linear ordinary differential equations using transformation of variables. Numerical computational is implemented for coupled nonlinear equations using finite difference method (FDM) to analyze the flow and heat transfer characteristics under the influence of various physical parameters namely: Prandtl fluid parameter, elastic parameter, magnetic parameter, stagnation parameter, Prandtl number, Brownian motion parameter, thermophoresis parameter, Lewis number, stretching parameter, and Biot number. Obtained results describe the effects of significant parameters on temperature and nanoparticle volume concentration due to zero flux and convective boundary condition. It is found that due to zero flux, concentration of nanoparticles disperse at the surface within the boundary layer region.

Keywords: nanofluid, convective heat transfer, Prandtl fluid model, zero flux, numerical solution.

1. Introduction

Two major classifications of fluids are Newtonian and non-Newtonian fluids. The later differs from the former in a way that stress-strain relationship is not linear. We are circumscribed by numerous such kinds of fluids that possess nonlinear stress-strain relationship. The applications lie in the range of fields from our daily life to industry. Based upon high viscosity few daily used non-Newtonian fluids are: toothpaste, ketchup, honey, paint, plastic, syrup, etc. Keeping view of such important usage the researchers have studied various aspects of non-Newtonian fluid by considering different model fluids, such as, power law fluid [1, 2], Prandtl fluid [3-5], and second grade fluid [6, 7].

Nanofluids are the kind of fluid which is a composite of nanometer-sized (around 1-100 nm) particles (metals, semiconductors, carbon nanotubes, etc.) and base fluids (water, glycol, engine oil, etc.). Such kind of fluids have revolutionized present era due to its marvelous applications in a way that, in comparison to conventional base fluids, they help in enhancing the heat transfer rate and thermal conductivity [8, 9]. It has been used is variety of engineering and medical fields, like, in nuclear reactors, where nanofluids serve as coolants due to their high thermal conductivity; in extraction of geothermal energy from the earth's crust having really high temperature ranges from 500^{o}C to 1000^{o}C, where the nanofluids having superconductivity may be used to extract geothermal energy to meet the energy need of world; in automobiles, where with the use of nanofluids the aerodynamics of automobiles may be improved resulting in reduced friction, economical fuel consumption and improved performance; in biomedical applications, where with the proper use of nanofluids the drug may improve its performance by targeting directly to the area of interest while reducing the side effects by not affecting other parts, are few of them. For more detailed applications readers are referred to [10]. Therefore recently it has become a very demanding area of research due to nanotechnology. Moreover, the study of nanofluid at stretching surface in specific has been the area of interest for many researchers. Few recent studies that deals the heat transfer analysis in the absence and presence of nanoparticles are [11-28]

The term convective heat transfer is simply referred to as heat transfer through convection. That is, when a fluid flows past a solid surface and heat is transferred between fluid and the surface. Such kind of heat transfer has vast applications. Foremost examples included: baking of breads and cookies, making of ice-cream, preserving food stuff in cold chiller rooms, etc. Having such important importance in our daily life, convective heat transfer over different types of surfaces has been studied in past. Recently convective heat transfer of carbon nanotubes tubes based nanofluid flow over stretching sheet was studied by Noreen et al. [29]. Two-dimensional and three-dimensional non-Newtonian nanofluid over stretching surface was explored by S. Nadeem et al. [30-34]. In another study, Shehzad e al. [35] discussed the 2-D stagnation point flow of Jeffry fluid to analyze the Soret and Dufour effects on fluid characteristics. For detailed study of convective heat transfer, readers are referred to [36].

As discussed in details in the above sections that the study of nanofluid has already benefited in versatile areas in engineering and medical sciences, many of its aspects are still yet to be discovered to meet the requirements of future needs. Main purpose of present paper is to study non-Newtonian type of fluid flow by considering Prandtl fluid model over convective stretching sheet where zero normal flux of nanoparticles is considered. All the governing equations are analyzed numerically and useful results are presented and discussed through numbers and graphs. The paper is distributed in various sections as: section 1 gives insight into the existing literature and motivation towards the present research work; section 2 is devoted to model the governing equations and convert them to suitable form for numerical experiment; section 3 presents and discusses the useful results; section 4 gives the precise conclusion of the present research work. All the cited references are listed in reference section.

2. Mathematical Framework

Let us consider 2-D stagnation point flow of a Prandtl fluid flow over a convective stretching surface. The fluid is incompressible, steady and confined to Cartesian plane $(y > 0)$. Fluid flows along positive y-axis and meets the plane $y = 0$. Surface is stretched with linear constant velocity and uniform magnetic field is applied normal to it. The stress tensor defined for Prandtl fluid is given by [3-5]:

$$\tau = \frac{A \arcsin\left(\frac{1}{C}\left(\left(\frac{\partial \bar{u}}{\partial y}\right)^2 + \left(\frac{\partial \bar{v}}{\partial x}\right)^2\right)^{1/2}\right)}{\left(\left(\frac{\partial \bar{u}}{\partial y}\right)^2 + \left(\frac{\partial \bar{v}}{\partial x}\right)^2\right)^{1/2}} \frac{\partial \bar{u}}{\partial y}, \tag{1}$$

Where, A and C are the material constants of Prandtl fluid model. After necessary boundary layer approximation, governing equations involved with the Brownian and thermophoresis are described as follows [12]:

$$\frac{\partial u}{\partial x} + \frac{\partial u}{\partial y} = 0, \tag{2}$$

$$u\frac{\partial u}{\partial x} + v\frac{\partial u}{\partial y} = u_\infty \frac{\partial u_\infty}{\partial x} - \frac{\sigma B_0^2}{\rho}(u - u_\infty) + \frac{\vartheta A}{C_1}\frac{\partial^2 u}{\partial y^2} + \frac{\vartheta A}{2C_1^3}\left(\frac{\partial u}{\partial y}\right)^2 \frac{\partial^2 u}{\partial y^2}, \tag{3}$$

$$u\frac{\partial T}{\partial x} + v\frac{\partial T}{\partial y} = \alpha\left(\frac{\partial^2 T}{\partial y^2}\right) + \tau_T D_B \frac{\partial C}{\partial y}\frac{\partial T}{\partial y} + \left(\sqrt{\frac{\tau D_T}{T_\infty}}\frac{\partial T}{\partial y}\right)^2, \tag{4}$$

$$u\frac{\partial C}{\partial x} + v\frac{\partial C}{\partial y} = D_B\left(\frac{\partial^2 C}{\partial y^2}\right) + \frac{D_T}{T_\infty}\left(\frac{\partial^2 T}{\partial y^2}\right), \tag{5}$$

where u, u_∞, v, T, T_w, T_∞, C, C_w and C_∞ denote the velocity of fluid in $x-$ direction, ambient fluid velocity, velocity of fluid in $y-$direction, temperature of fluid, temperature of fluid at the stretching surface, ambient fluid temperature, nanoparticle volume concentration, nanoparticle concentration at the stretching surface and nanoparticle concentration at the ambient fluid, respectively, ϑ denote the kinematic viscosity of the fluid, σ is the electrical conductivity, ρ is the density of fluid, α represents the thermal diffusivity of fluid, $\tau_T = (\rho c)_p / (\rho c)_f$ represents the ration of heat capacity of the particle to heat capacity of the fluid, D_T and D_B represent the thermophoretic diffusion coefficient and Brownian diffusion coefficient, respectively. The boundary conditions for equations (2)–(5) are set as:

$$\left.\begin{array}{l} u = u_w(x) = cx, \quad v = 0, \quad -k_f \dfrac{\partial T}{\partial y} = h_f (T_f - T), \\ D_B \dfrac{\partial C}{\partial y} + \dfrac{D_T}{T_\infty} \dfrac{\partial T}{\partial y} = 0, \end{array}\right\} \text{at } y = 0, \tag{6}$$
$$u = u_\infty(x) = bx, \; v = 0, \; T = T_\infty, \; C = C_\infty \text{ as } y \to \infty.$$

In Eq.(6), expression $D_B \dfrac{\partial C}{\partial y} + \dfrac{D_T}{T_\infty} \dfrac{\partial T}{\partial y} = 0$ is used for zero normal flux. Where, $u_w(x)$ and $u_\infty(x)$ are the velocity of the sheet at wall and free stream velocity of the fluid. By using the similarity transformations to convert the above partial differential equations (2)–(6) into ordinary differential equations:

$$\psi = (a\vartheta)^{1/2} x f(\eta) \;\;,\;\; \theta(\eta) = \frac{T - T_\infty}{T_w - T_\infty} \;\;,\;\; \phi(\eta) = \frac{C - C_\infty}{C_w - C_\infty} \;,\;\; \eta = \sqrt{\frac{a}{\vartheta}} y. \tag{7}$$

Where, velocities $u = \partial\psi/\partial y$ and $v = -\partial\psi/\partial x$ are defined in term of stream function ψ. Using the definition of stream function ψ it can be verified easily that Eq. (2) identically satisfied the law of conservation of mass and Eqs. (3)-(5) along with relevant boundary conditions defined in Eq. (6) are converted into the following form:

$$\alpha f'''(\eta) + f(\eta) f''(\eta) - \left(f'(\eta)\right)^2 + \beta f'''(\eta)\left(f''(\eta)\right)^2 + M\left(r - f'(\eta)\right) + r^2 = 0, \tag{8}$$

$$\frac{1}{\Pr}\theta''(\eta) + f(\eta)\theta'(\eta) + Nb\theta'(\eta)\phi'(\eta) + Nt\left(\theta'(\eta)\right)^2 = 0, \tag{9}$$

$$\phi''(\eta) + Le\Pr f(\eta)\phi'(\eta) + \frac{Nt}{Nb}\theta''(\eta) = 0, \tag{10}$$

The dimensionless form of boundary conditions relative to the defined model is,

$$\left.\begin{array}{l} f(0) = 0, \;\; f'(0) = \lambda, \;\; f'(\eta \to \infty) = r, \\ \theta'(0) = -Bi(1 - \theta(0)), \quad \theta(\eta \to \infty) = 0, \\ Nb\phi'(0) + Nt\theta'(0) = 0, \;\; \phi(\eta \to \infty) = 0. \end{array}\right\} \tag{11}$$

where, prime indicates the differentiation with respect to η, where $\alpha = A/C_1$ is Prandtl fluid parameter, $\beta = a^3 x^2 A / 2C_1^3 \vartheta$ is elastic parameter, $r = b/a$ is the stagnation parameter, $\lambda = c/a$ is the stretching $(\lambda > 0)$ or shrinking $(\lambda < 0)$ parameter, $\Pr = \vartheta/\alpha$ is Prandtl number, $M = \sigma B_0^2/\rho a$ is magnetic parameter, $Le = a/D_B$, $Nb = \dfrac{(\rho c)_p D_B (C_w - C_\infty)}{\nu(\rho c)_f}$, and $Nt = \dfrac{(\rho c)_p D_T (T_w - T_\infty)}{\nu T_\infty (\rho c)_f}$ are the Lewis number, Brownian motion, and thermophoresis parameter, respectively. Friction and heat transfer at the surface are defined as:

$$C_f = \frac{\tau_w}{\rho u_w^2}, \quad Nu = \frac{x q_w}{\alpha (T_w - T_\infty)}, \tag{12}$$

Where, τ_w and q_w are the stress tensors and heat flux, respectively:

$$\tau = \frac{A}{C}\frac{\partial u}{\partial y} + \frac{A}{6C^3}\left(\frac{\partial u}{\partial y}\right)^3, \quad q_w = -\alpha\left(\frac{\partial T}{\partial y}\right)_{y=0}, \tag{13}$$

Dimensionless form of equation (13) take the form:

$$\sqrt{\mathrm{Re}}\, c_f = \left[\alpha f''(\eta) + \beta\left(f''(\eta)\right)^3\right]_{\eta=0}, \quad \mathrm{Re}_x^{-1/2} Nu = -\theta'(0). \tag{14}$$

where, $\mathrm{Re}_x = \dfrac{u_w x}{\vartheta}$ is local Reynolds number.

3. Methodology

Numerical simulation is performed over system off non-linear coupled Eqs. (8)-(10) along with the associated boundary conditions defined in Eq. (11) using finite difference method. The uniform step size of 10^{-4} and truncation error tolerance of 10^{-8} was used. After initial experimental analysis it was concluded to restrict the infinite domain to η = [0, 20] to show the convergence of the solution profiles. The obtained useful results are discussed in the following paragraphs. Table 1, shows the validation of present study with the result published by Khan and Pop [12]. In this comparison, results are produce in the absence of zero normal flux so we have used the expression for Sherwood number is $\mathrm{Re}_x^{-1/2} Sh = -\phi'(0)$.

Table 1 : Comparison of numerical values for $\mathrm{Re}_x^{-1/2} Nu_x$ and $\mathrm{Re}_x^{-1/2} Sh$ for constant wall temperature when $\Pr = 10$ and $Le = 1$.

$\alpha = \lambda = 1,\ \beta =$ M=$r = 0,\ \mathrm{Bi} \to \infty$	Present results	Present results	Khan [12]	Khan [12]
Nt	$-\theta'(0)$	$-\phi'(0)$	$-\theta'(0)$	$-\phi'(0)$
0.1	0.9524	2.1294	0.9524	2.1294
0.2	0.6932	2.2732	0.6932	2.2740
0.3	0.5201	2.5286	0.5201	2.5286
0.4	0.4026	2.7952	0.4026	2.7952
0.5	0.3211	3.0351	0.3211	3.0351

4. Results and discussion

Figures 1 and 2 depicts the velocity profiles $f'(\eta)$ of fluid under the change of involved physical parameters, that are, Prandtl fluid parameter α, Magnetic parameter M, stretching parameter λ, stagnation parameter r and elastic parameter β. Figure 1(a) shows that the due to increase in Prandtl fluid parameter α fluid velocity $f'(\eta)$ tends to increase for stretching surface $\lambda > 0$ whereas inverse profiles was observed in the case of shrinking sheet $\lambda < 0$. Looking at figure 1(b) we can see that due to increase in magnetic parameter M the fluid velocity $f'(\eta)$ tends to decrease in the case of stretching sheet $\lambda > 0$ whereas inverse behavior is observed in the case of shrinking case $\lambda < 0$. The velocity boundary layer thickness tends to decreases by increase in magnetic M and Prandtl fluid parameter α. Figure 2(a) shows the effects of stagnation parameter r over fluid velocity $f'(\eta)$ over stretching $\lambda > 0$ and shrinking sheet $\lambda < 0$. It can be seen clearly that velocity $f'(\eta)$ tends to increase for both stretching and shrinking cases, as the value of stagnation r parameter increases. Figure 2(b) shows that both velocity $f'(\eta)$ and boundary layer thickness tends to decrease due to increase in elastic β parameter for $\lambda > 0$ and $\lambda < 0$. It is further noted that the velocity for the stretching $\lambda > 0$ is more than the shrinking case $\lambda < 0$.

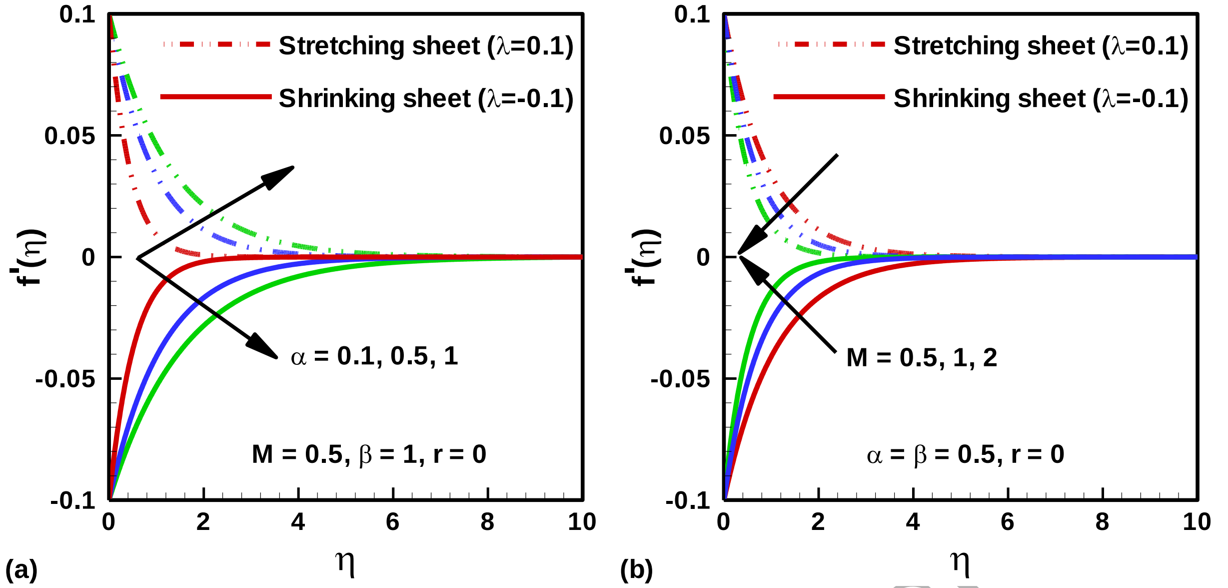

Figure 1: Effects of Prandtl fluid α and magnetic M parameter over fluid velocity $f'(\eta)$.

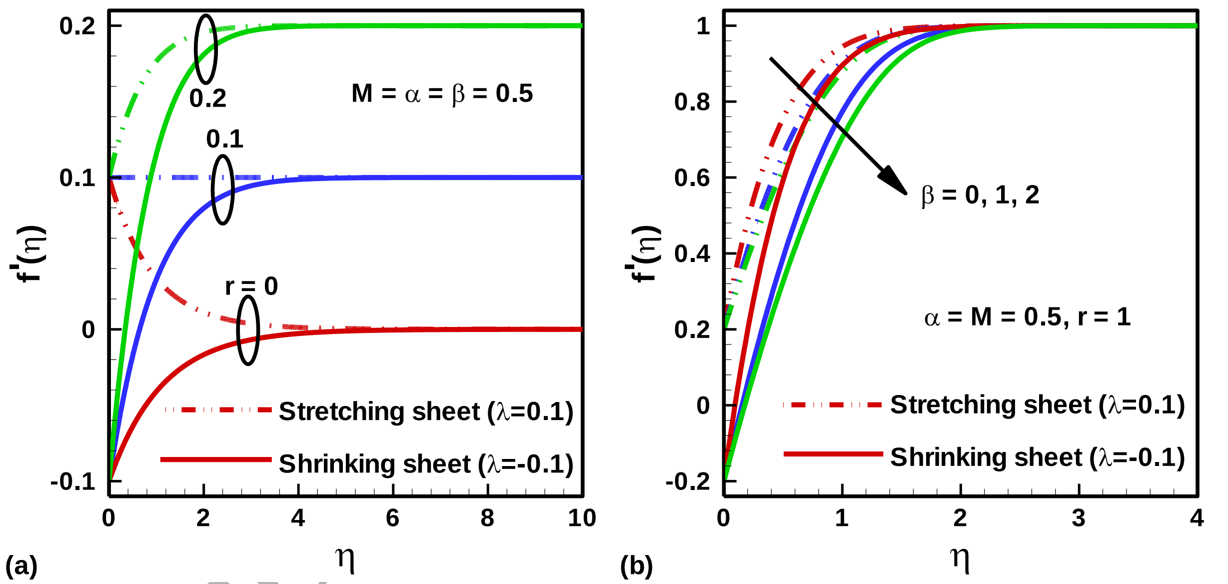

Figure 2: Effects of stagnation r and elastic β parameter over fluid velocity $f'(\eta)$.

Figure 3 and 4 depicts the effects of involved physical parameters on the fluid temperature $\theta(\eta)$. Figure 4(a) shows that temperature $\theta(\eta)$ is increased due to increase in Prandtl fluid parameter α. Moreover temperature $\theta(\eta)$ is noticed to be higher on shrinking sheet $\lambda<0$ than stretching sheet $\lambda>0$. Figure 3(b) shows that the temperature $\theta(\eta)$ and thicknesses of boundary layer is declined due to increase in Prandtl number $\Pr$ for $\lambda>0$ and $\lambda<0$. It was also noticed that temperature is lower for stretching sheet $\lambda > 0$ than of shrinking sheet $\lambda < 0$. Figure 4(a) shows that temperature increases $\theta(\eta)$ due to increase in Biot number Bi whereas thermal boundary layer thickness is decreased. The temperature for shrinking case $\lambda < 0$ is greater than the stretching case $\lambda > 0$ for various values of thermophoresis parameter. Figure 4(b) shows the temperature distribution decreases due to increase in thermophoresis parameter Nt in the case of shrinking sheet $\lambda < 0$ whereas inverse behavior was observed in the cases of stretching sheet $\lambda > 0$.

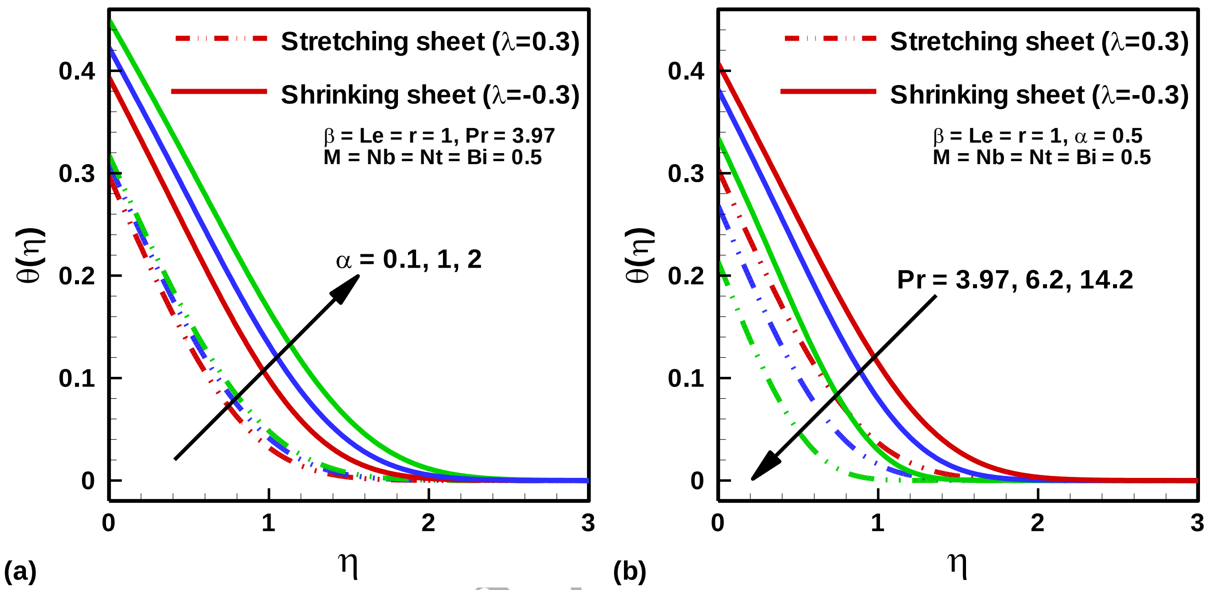

Figure 3: Variation of $\theta(\eta)$ for various values of Prandtl fluid parameter and Prandtl number $\Pr$.

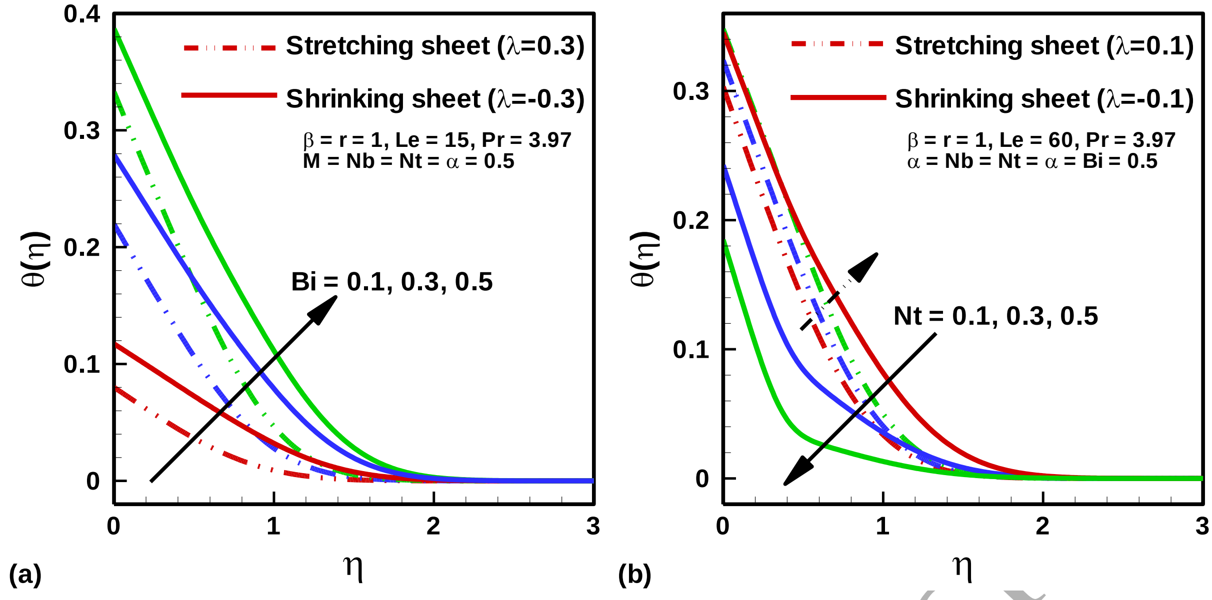

Figure 4: Variation of $\theta(\eta)$ for various values of Biot number Bi and thermophoresis parameter Nt.

Figure 5 shows that variation in shear stress due to various physical parameters involved. It is shown by figure 5(a)–5(c) that skin friction coefficient always tends to decreases by increasing stretching parameter λ. It is also noted that, by increasing the vales of magnetic parameter M, elastic parameter β and stagnation parameter r increases the friction with the wall. Whereas skin friction decreases by increasing Prandtl fluid parameter α. Figures 6 and 7 demonstrate the variation of Nusselt number due to change in involved physical parameters. It is noticed that Nusselt number always tends to increases due to increase in stretching parameter λ. Figure 6(a) shows that Nusselt number decreases due to increases in elastic parameter β and Prandtl fluid parameter α whereas inverse profile was observed for increasing value of magnetic parameter M. The Figure 7(a) shows very interesting behavior of Nusselt number where Nusselt number tends to increase due to increases in thermophoresis parameter Nt where stretching parameter λ has value less than or equal to -0.5 and inverse profiles are obtained when stretching parameter λ value is greater than -0.5. Figure 7(b) shows that increasing Prandtl parameter α and Biot number Bi increases Nusselt number. Figure 8 shows that graphical representation of streamlines for various values of shrinking parameter $\lambda < 0$.

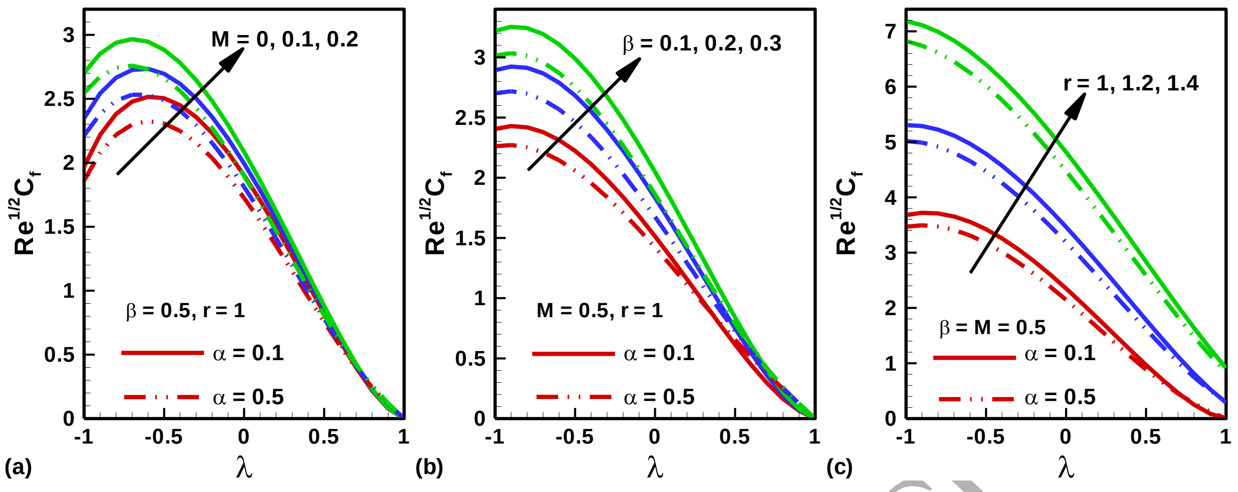

Figure 5: Effects of magnetic M, elastic β and stagnation r parameter over skin friction coefficient.

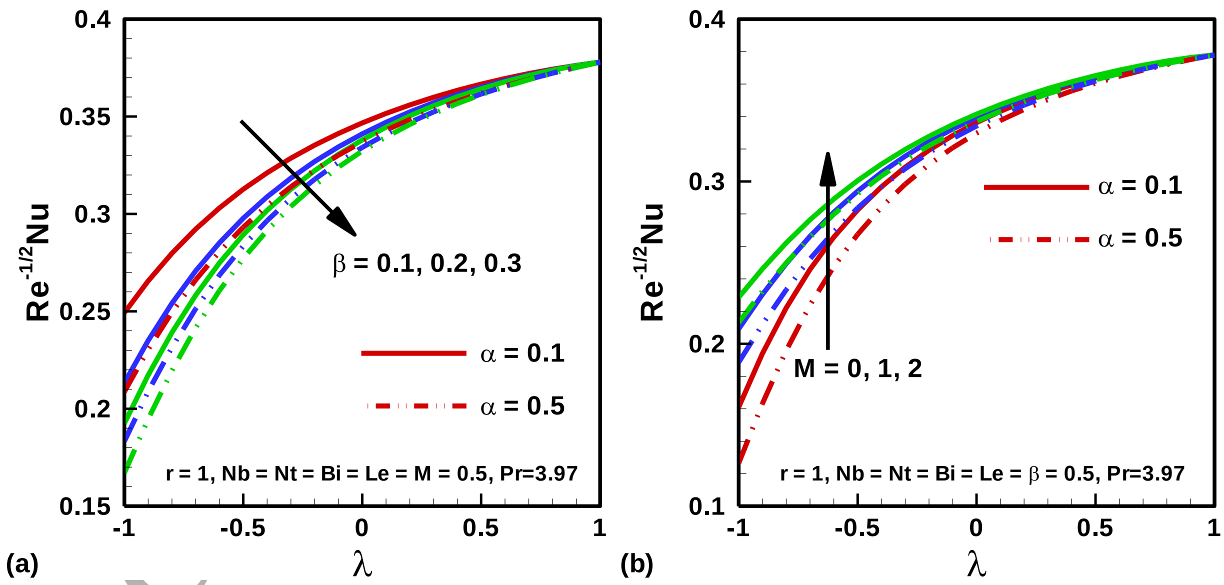

Figure 6: Effects of elastic β and magnetic M parameter over Nusselt number.

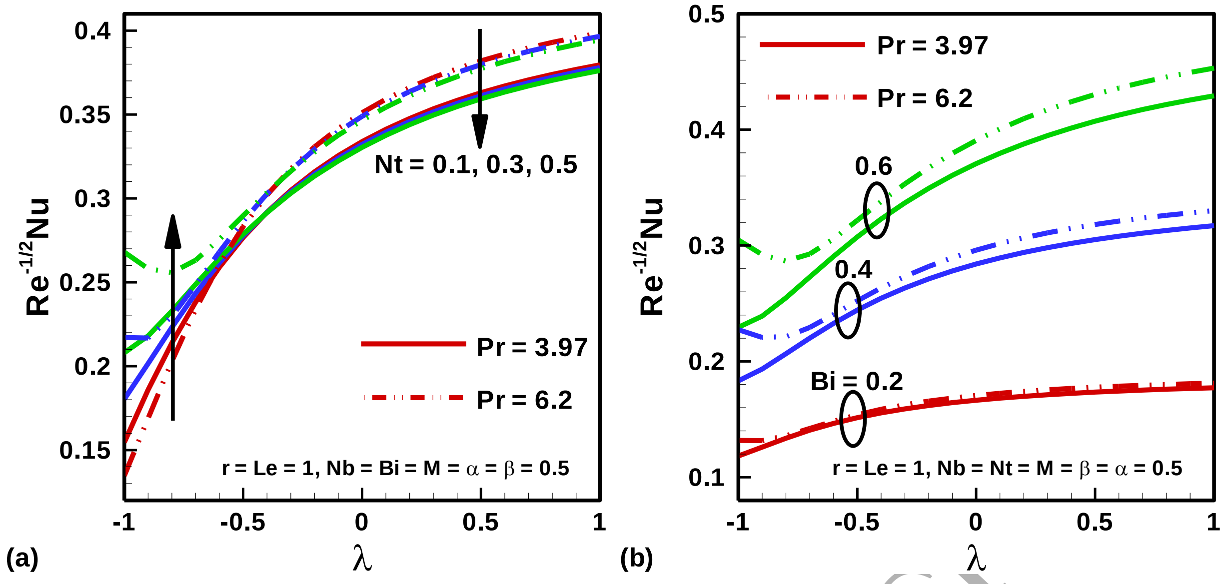

Figure 7: Effects of thermophoresis Nt, Biot Bi and Prandtl number $\Pr$ over Nusselt number.

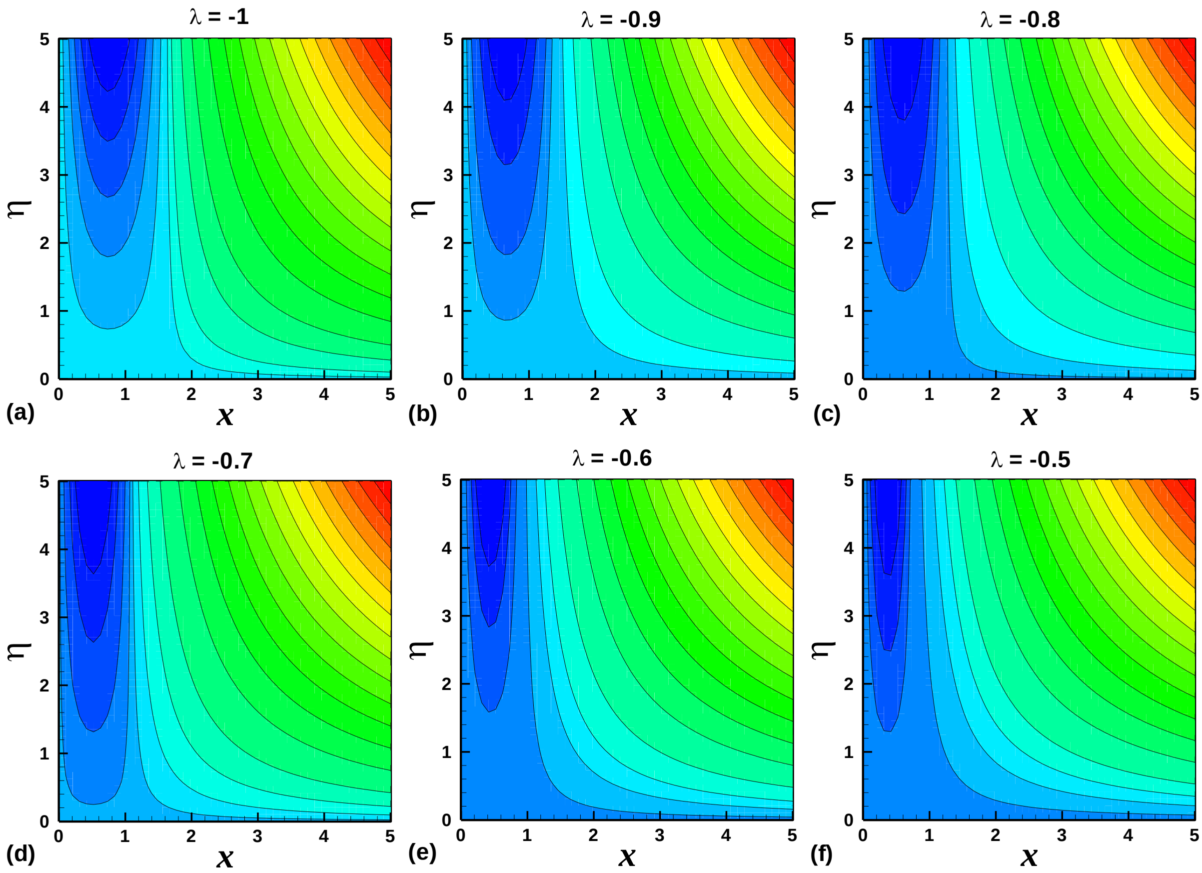

Figure 8. Flow streamlines for various values of stretching parameter λ.

5. Conclusion

Study of stagnation point flow of non-Newtonian (Prandtl fluid model) is deal in the presence of nanoparticles over a convectively surface. Moreover, zero normal flux of nanoparticles was studied in this paper. The effects of contained physical parameters namely:, Prandtl fluid parameter α, elastic parameter β, magnetic parameter M, stagnation parameter r, Prandtl number $\Pr$, Brownian motion Nb, thermophoresis Nt, Lewis number Le, stretching parameter λ, and Biot number Bi, on the quantities of interests: fluid velocity, temperature, skin friction and heat transfer rate were analyzed in details. It is found that for stretching sheet $\lambda > 0$ fluid velocity $f'(\eta)$ increases due to increase in α whereas decreases due to increase in M. For shrinking sheet $\lambda < 0$, fluid velocity tends to decrease due to increase in α and increases due to increase in magnetic parameter M. For both stretching and shrinking cases, fluid velocity $f'(\eta)$ increases due to increase in stagnation parameter r whereas it decreases due to increase in elastic parameter β. For both stretching $\lambda > 0$ and shrinking $\lambda < 0$ sheet, the fluid temperature $\theta(\eta)$ is increased due to increase in Prandtl fluid α parameter and Biot number Bi whereas decreases due to increase in Prandtl number $\Pr$. Fluid temperature $\theta(\eta)$ also increases due to increase in thermophoresis Nt parameter for stretching case while it decreases for shrinking case. Wall skin friction was reduced due to increase in Prandtl fluid parameter α and stretching parameter λ however, it increases due to increase in magnetic M, elastic β and stagnation parameters r. Wall heat transfer rate is increased due to increase in stretching λ, magnetic M, Prandtl $\Pr$ parameters and Biot Bi number and reduced due to increase in Prandtl fluid α, elastic β and thermophoresis Nt parameter.

Acknowledgements

First and the last authors are thankful to National Science Foundation of China (NSFC) for financially supported having grant number 11671199.

6. References

[1] Y. Lin, L. Zheng and Lianxi Ma, Heat transfer characteristics of thin power law liquid films over horizontal stretching sheet with internal heating and variable thermal coefficient, Applied Mathematics and Mechanics, 37(12) (2016) 1587-1596.

[2] J. Ahmed, T. Mahmood, Z. Iqbal, A. Shahzad and R. Ali, Axisymmetric flow and heat transfer over an unsteady stretching sheet in power law fluid, Journal of Molecular Liquids, 221 (2016) 386-393.

[3] N. S. Akbar, Z. H. Khan, R. U. Haq and S. Nadeem, Dual solutions in MHD stagnation-point flow of Prandtl fluid impinging on shrinking sheet, Applied Mathematics and Mechanics, 35(7) (2014) 813-820.

[4] N. S. Akbar, Blood flow analysis of Prandtl fluid model in tapered stenosed arteries, Ain Shams Engineering Journal, 5 (2014) 1267-1275.

[5] S. Nadeem, S. Ijaz and N. S. Akbar, Nanoparticle analysis for blood flow of Prandtl fluid model with stenosis, International Nano Letters, 3(35) (2013).

[6] T. Hayat, A. Aziz, T. Muhammad and B. Ahmed, On magnetohydrodynamic flow of second grade nanofluid over a nonlinear stretching sheet, Journal of Magnetism and Magnetic Materials, 408 (2016) 99-106.

[7] M. Khan and M. U. Rahman, Flow and heat transfer to modified second grade fluid over a nonlinear stretching sheet, AIP Advances, 5 (2015) 087157.

[8] K. Kwak and C. Kim, Viscosity and thermal conductivity of copper oxide nanofluid dispersed in ethylene glycol, Korea-Australia Rheology Journal, 17(2) (2005) 35-40.

[9] S. U. S. Choi and J. A. Eastman, Enhancing thermal conductivity of fluids with nanoparticles, ASME International Mechanical Engineering Congress and Exposition, November 12-17 (1995) San Francisco, CA.

[10] K. V. Wong and O. D. Leon, Applications of nanofluids: current and future, Advances in Mechanical Engineering, (2010) e519659.

[11] J. Buongiorno, Convective transport in nanofluids, Journal of Heat Transfer, 128(3) (2006) 240-250.

[12] W. A. Khan and I. Pop, Boundary-layer flow of a nanofluid past a stretching sheet. International journal of heat and mass transfer, 53 (2010) 2477-2483.

[13] S. Moein, M. Rassoulinejad and S. Abbasbandy, Analysis of forced convection in a circular tube filled with a Darcy-Brinkman-Forchheimer porous medium using spectral homotopy analysis method, Journal of Fluids Engineering, 133(10) (2011) e101207.

[14] S. Munawar; A. Mehmood and A. Ali, Time-dependent flow and heat transfer over a stretching cylinder, Chinese Journal of Physics, 50 (2012) 828-848.

[15] H. A. Attia, L. A-Hassan, M. A. M. Abdeen, A. El-Din Abdin, W. Abd El-Meged, Unsteady couette flow of a thermally conducting viscoelastic fluid under constant pressure gradient in a porous medium, Chinese Journal of Physics, 52(3) (2014)1015-1027.

[16] Y. Shagaiya Daniel, Z. A. Aziz, Z. Ismail, F. Salah, Effects of thermal radiation, viscous and Joule heating on electrical MHD nanofluid with double stratification, Chinese Journal of Physics, 55(3) (2017) 630-651.

[17] S. Saleem, M. Awais, S. Nadeem, N. Sandeep, T. Mustafa, Theoretical analysis of upper-convected Maxwell fluid flow with Cattaneo-Christov heat flux model, Chinese Journal of Physics, (2017). doi.org/10.1016/j.cjph.2017.04.005.

[18] S. M. R-Mousavi, H. R. Seyf and S. Abbasbandy, Heat transfer through a porous saturated channel with permeable walls using two-equation energy model, Journal of Porous Media, 16(3) (2013) 241-254.

[19] S. M. R-Mousavi, S. Abbasbandy and H. H. Alsulami, Analytical flow study of a conducting Maxwell fluid through a porous saturated channel at various wall boundary conditions, European Physical Journal Plus, 129 (2014) e181.

[20] S. M. R-Mousavi amd H. Yaghoobi, Effect of non-linear drag term on viscous dissipation in a fluid saturated porous medium channel with various boundary conditions at walls, Arabian Journal for Science and Engineering, 39(2) (2014) 1231–1240.

[21] S. U. Rahman, R. Ellahi, S. Nadeem and Q. M. Z. Zia, Simultaneous effects of nanoparticles and slip on Jeffrey fluid through tapered artery with mild stenosis, Journal of Molecular Liquids, 218 (2016) 484-493.

[22] M. Sheikholeslami and R. Ellahi, Three dimensional mesoscopic simulation of magnetic field effect on natural convection of nanofluid, International Journal of Heat and Mass Transfer, 89 (2015) 799-808.

[23] R. Ellahi, M. Hassan and A. Zeeshan, Shape effects of nanosize particles in Cu-H_2O nanofluid on entropy generation, International Journal of Heat and Mass Transfer, 81 (2015) 449-456.

[24] Z. Liu, Y. Liu, Y. Chang, H. R. Seyf, A. Henry, A. L. Mattheyses, K. Yehl, Y. Zhang, Z. Huang and K. Salaita, Nanoscale optomechanical actuators for controlling mechanotransduction in living cells, Nature methods, 13(2) (2016) 143-146.

[25] S. M. R-Mousavi, Y. Mao and Y. Zhang, Evaluation of copper, aluminum, and nickel interatomic potentials on predicting the elastic properties, Journal of Applied Physics, 11 (2016) e244304.

[26] A. Zeeshan, A. Majeed and R. Ellahi, Effect of magnetic dipole on viscous ferro-fluid past a stretching surface with thermal radiation, Journal of Molecular Liquids, 215 (2016) 549-554.

[27] R. Ellahi, M. Hassan and A. Zeeshan, Aggregation effects on water base Al_2O_3-nanofluid over permeable wedge in mixed convection, Asia-Pacific Journal of Chemical Engineering, 11(2) (2016) 179-186.

[28] M. Sheikholeslami, Q. M. Z. Zia, R. Ellahi, Influence of induced magnetic field on free convection of nanofluid considering Koo-Kleinstreuer-Li (KKL) correlation, Applied Sciences, 6(11) (2016) e324.

[29] N. S. Akbar, Z. H. Khan and S. Nadeem, The combined effects of slip and convective boundary conditions on stagnation point flow of CNT suspended nanofluid over a stretching sheet, Journal of Molecular Liquids, 196 (2014) 21-25.

[30] S. Nadeem, R. U. Haq, N. S. Akbar, C. Lee and Z. H. Khan. Numerical study of boundary layer flow and heat transfer of Oldroyd-B nanofluid towards a stretching sheet. PLoS ONE, 8(8) (2013) e69811.

[31] S. Nadeem, R. U. Haq and Z. H. Khan, Numerical study of MHD boundary layer flow of a Maxwell fluid past a stretching sheet in the presence of nanoparticles, Journal of the Taiwan Institute of Chemical Engineers, 45(1) (2014) 121-126.

[32] S. Nadeem, R. U. Haq and N. S. Akbar, MHD three-dimensional boundary layer flow of Casson nanofluid past a linearly stretching sheet with convective boundary condition, IEEE Transactions on Nanotechnology, 13(1) (2014) 109-115.

[33] S. Nadeem, R. U. Haq and Z. H. Khan, Numerical solution of non-Newtonian nanofluid flow over a stretching sheet, Applied Nanoscience, 4(5) (2014) 625-631.

[34] S. Nadeem and R. U. Haq, Effect of thermal radiation for magneto-hydrodynamic boundary layer flow of a nanofluid past a stretching sheet with convective boundary conditions, Journal of Computational and Theoretical Nanoscience, 11(1) (2014) 32-40.

[35] S. A. Shehzad, F. E. Alsaedi, S. J. Manaquel and T. Hayat, Soret and dufour effects on the stagnation-point flow of Jeffry fluid with convective boundary condition, European Physical Journal Plus, 128 (2013) e56.

[36] A. Bejan, Convection Heat Transfer, third edition, Wiley, Hoboken, (2004) 586– 591.

Graphical Abstract

Model is intended to describe the variations of skin friction for various values of emerging parameters and behavior of stream lines for shrinking case.